CMS Physics Analysis Summary

Contact: cms-pag-conveners-bphysics@cern.ch 2025/04/07

Observation of X(6900) and evidence for X(7100) in the $J/\psi\psi(2S) \to \mu^+\mu^-\mu^+\mu^-$ mass spectrum in 314 fb^{-1} of pp collisions at CMS

The CMS Collaboration

Abstract

A search is performed for structures near threshold in the $J/\psi\psi(2S) \to \mu^+\mu^-\mu^+\mu^-$ channel using a sample of proton-proton collisions at $\sqrt{s} = 13.0$ TeV and 13.6 TeV recorded by the CMS detector at the CERN LHC. The data correspond to an integrated luminosity of about 314 fb^{-1}. A threshold structure is observed near 6900 MeV with a significance in excess of five standard deviations ($>5\sigma$), and there is also evidence (4.0σ) for a second peak, in a model where the structures mutually interfere. The mass and width of the two peaks are measured to be $6876^{+46\,+110}_{-29\,-110}$, $253^{+290\,+120}_{-100\,-120}$ MeV and $7169^{+26\,+74}_{-52\,-70}$, $154^{+110\,+140}_{-82\,-160}$ MeV, which are consistent to within one standard deviation of the X(6900) and X(7100) structures previously observed in the $J/\psi J/\psi$ spectrum.

The CMS Collaboration has reported a triplet of structures in the J/ψJ/ψ mass spectrum, labeled as X(6600), X(6900), and X(7100) [1, 2]. CMS data favored a model where the three objects quantum mechanically interfere with each other, implying that they all have the same J^{PC}. The relatively large mass splittings ($\gtrsim$200 MeV) between members suggests that these may be a family of radial excitations [3–5]. These structures are candidates for a family of all-charm tetraquarks.

Tetraquarks became a topic of intense interest in the wake of the discovery of the $\chi_c(3872)$ meson by the Belle Collaboration in 2003 [6]. Seen in the J/$\psi\pi^+\pi^-$ channel, this state did not conform to the expectations for charmonia. Unequivocal evidence for non-$q\bar{q}$ mesons was obtained by the Belle and BESIII Collaborations in 2013 with the discovery of a charged charmonium-like state $Z_c^+(3900) \to$ J/$\psi\pi^+$ [7, 8].

Many candidates for exotic hadrons—states other than $q\bar{q}$ and qqq—are now known [9, 10]. However, prior to the discovery of the J/ψJ/ψ structures [1, 2, 11, 12], they all contained light quarks, and the characterization of their internal structure has been debated. Tetraquarks have been modeled as molecular states of conventional mesons [13–15], diquark-antidiquark systems [4, 16, 17], and gluonic hybrids of tetraquarks [18]. Some of the observed states have been considered as compact states [19]. It has even been argued that many exotic candidates may arise from dynamical effects of production thresholds: coupled-channel interactions [20], triangle singularities [21], or Pomeron exchange [18, 22, 23]. The prospect of exotics composed entirely of heavy (c, b) quarks holds the promise of providing clarity to the nature of multiquark exotic meson states.

A step towards the observation of systems composed of only heavy quarks was the CDF Collaboration's report of $Y(4140)\to$J/$\psi\phi$ decays in 2009 [24, 25]—providing the first candidate for a $c\bar{c}s\bar{s}$ state. Then, in 2020, the LHCb Collaboration discovered the X(6900) structure in the J/ψJ/ψ mass spectrum [11], providing the first candidate for a fully-heavy tetraquark. This structure is now well-established with confirmations by the ATLAS and CMS Collaborations [1, 2, 12].

While the J/ψJ/ψ spectrum has yielded important advances, the spectrum remains enigmatic with ATLAS, CMS, and LHCb all having reported additional features for which there is not yet concensus [1, 2, 11, 12]. Further experimental study is crucial to unravel the underlying physics.

This note extends our study of all-charm exotics to the J/$\psi\psi(2S)\to\mu^+\mu^-\mu^+\mu^-$ channel, where an X(6900) peak would be at threshold.

ATLAS has already reported a significant near-threshold excess in this channel [12]. However, details of the structure(s) could not be unequivocally discerned from their data, and they refrained from specifically characterizing their excess. Two fit models were offered. Model α consisted of an X(6900) resonance (including the tails of two sub-threshold resonances) with parameters fixed to the values from their J/ψJ/ψ data [12], plus a (non-interfering) resonance above the X(6900) peak. The latter gave a mass and width of $7220 \pm 30^{+10}_{-40}$ and $90 \pm 60^{+60}_{-30}$ MeV (throughout this note, if two uncertainties are given the first is statistical and the second systematic, whereas if a single uncertainty is given, it is the statistical uncertainty only). The collective significance of the threshold structure was 4.7 standard deviations (4.7σ), and the 7220 MeV structure's local significance was 3.0σ. Model β had a single broad resonance (which absorbed the excess of events near 7220 MeV), yielding a mass and width of $6960 \pm 50 \pm 30$ and $510 \pm 170^{+110}_{-100}$ MeV. These results need clarification.

Our J/$\psi\psi(2S)$ investigation uses a data set of 314 fb^{-1} of integrated luminosity of pp collisions

produced by the LHC, and collected over 2016-2018 (Run 2, 134.8 fb^{-1}, center-of-mass energy of 13 TeV) and 2022-2024 (Run 3, 179.6 fb^{-1}, center-of-mass energy of 13.6 TeV) using the CMS detector.

The central feature of the CMS apparatus is a superconducting solenoid of 6 m internal diameter and 13 m long, providing a magnetic field of 3.8 T. Within the solenoid volume are a silicon pixel and strip tracker, a lead tungstate crystal electromagnetic calorimeter, and a brass and scintillator hadron calorimeter, each composed of a barrel and two end-cap sections. Forward calorimeters extend coverage to high pseudorapidity. Muons are detected in gas-ionization chambers embedded in the steel flux-return yoke outside the solenoid. A detailed description of the CMS detector, including definitions of the coordinate system and the relevant kinematic variables used, can be found in Ref. [26].

Simulated samples are used to model signals and backgrounds. Signal samples of conventional $J^P = 0^+$ mesons of various masses decaying to J/$\psi\psi$(2S) were produced via gluon-gluon collisions by the JHUGen generator (version 7.40) [27–31]. Samples for non-resonant single-parton scattering (NRSPS) and non-resonant double-parton scattering (DPS) backgrounds were produced with the PYTHIA [32–37] package, and they include both direct production and feed-down processes producing J/ψ or $\psi(2S)$ mesons. Generated events are processed through the CMS detector simulation, based on GEANT4 [38].

Events of interest are collected using a two-tiered trigger system [39]. The first level (L1), composed of custom hardware processors, uses information from the calorimeters and muon detectors to select events. The second level, known as the high-level trigger (HLT), consists of a farm of processors running a faster version of the full offline event reconstruction software, and reduces the online event rate to around 1 kHz.

The data collected in 2016 correspond to an integrated luminosity of 36.3 fb^{-1}, and were obtained with an L1 trigger that required at least three muon candidates. The HLT required that the pseudorapidity of each muon satisfies $|\eta| < 2.5$, and that they contain a pair of oppositely charged muons with an invariant mass between 2.95 and 3.25 GeV, a distance of closest approach between the two muons less than 0.5 cm, and a fit to a common vertex with a χ^2 probability greater than 0.5%.

The data from 2017-2018 correspond to 98.4 fb^{-1}. Its L1 trigger required at least three muons with at least two having p_T>3 GeV and one of these having p_T>5 GeV, and at least one oppositely charged pair of muons with invariant mass below 9 GeV. The HLT criteria replicated those of 2016 with the additional requirement that the two muons with invariant mass between 2.95 and 3.25 GeV each have $p_\text{T} > 3.5$ GeV.

The data from 2022–2024 totaled 179.6 fb^{-1}. The L1 trigger replicated that of 2017–2018, but was supplemented by a parallel trigger only requiring at least two oppositely charged muon candidates—either trigger condition was sufficient for event selection. The HLT trigger demanded the oppositely charged pair of muons have a mass below 8.5 GeV; and that for the two muons selected, at least one muon has $p_\text{T} > 4$ GeV, and the other has $p_\text{T} > 3$ GeV.

The ψ(2S)$\to\mu^+\mu^-$ signal suffers from larger backgrounds and has a smaller branching fraction than for J/$\psi\to\mu^+\mu^-$, and a selection optimization is performed using 2016-18 data. The optimization uses the following selection parameters: the minimum of each of the $\psi(2S)$ and J/ψ p_T's, the minimum p_T of the muons from the $\psi(2S)$, the quality of the muon identification ("soft," "loose," or "medium" [40]) for the $\psi(2S)$, and the width of the J/ψ and $\psi(2S)$ mass windows. The values of all other parameters are taken from our J/ψJ/ψ analysis [1]. Selection parameters of interest are cycled through one at a time, and each parameter is stepped

through a range of values where we determine the number of signal S and background B candidates. S is the number of $X(6900)$ signal events from simulation and B is the number of background events from data in a 6.7-7.1 GeV mass window. A figure-of-merit (FOM) $S/(463/13 + 4\sqrt{B} + 5\sqrt{25 + 8\sqrt{B} + 4B})$ [41] is computed. The optimal point is chosen from the FOM scans for selected parameters, but rounded to 0.5 GeV increments for momentum-related variables to smooth out statistical fluctuations to protect against over-optimizing on them. Because the optimum of a one parameter scan may depend on the values of the other parameters, the cycle is repeated over all parameters until stable results are obtained.

The resulting selection is as follows. There must be four muons with zero net charge and satisfying: $p_T(J/\psi) > 11$ GeV; $p_T(\psi(2S)) > 13.5$ GeV; each $\psi(2S)$ muon satisfies CMS's "loose" muon identification criteria and has $p_T > 2.5$ GeV; and the dimuons must fall within a 2.5σ window of the known J/ψ or $\psi(2S)$ masses [42]. Finally, the four muons are fit to a common vertex, with opposite-sign pairs mass constrained to either the J/ψ or $\psi(2S)$ masses, and having a fit probability greater than 0.5% (roughly equivalent to the unconstrained mass being within 3σ of one of the ψ masses).

With a small $J/\psi\psi(2S)$ sample there are no multiple candidates per event, but because of the comparatively large $J/\psi J/\psi$ production, around 1% events reflect into our $J/\psi\psi(2S)$ sample due to the incorrect muon pairing. Therefore we veto $J/\psi\psi(2S)$ candidates that satisfy all criteria but have an alternate pairing of muons such that each pair falls within 2σ of the J/ψ mass.

A two-dimensional unbinned likelihood fit of the $\psi(2S)$ versus J/ψ candidate masses is performed on the final sample, yielding 386 ± 26 $J/\psi\psi(2S)$ signal pairs with pair masses below 15 GeV (109 ± 14 in Run 2 and 281 ± 22 in Run 3).

The resulting $J/\psi\psi(2S)$ mass distributions for different Runs are shown in Figure 1, whereas the combined fit to the data is presented in Figure 2. Similar to the $J/\psi J/\psi$ spectrum [1], a structure near a mass of 6900 MeV, close to the $J/\psi\psi(2S)$ threshold, is clearly seen and another structure near 7100 MeV is also seen.

The $J/\psi\psi(2S)$ spectrum is fit using the unbinned likelihood method with S-wave relativistic Breit-Wigner (BW) functions describing the two structures [42–44]. The NRSPS background shapes are parameterizations, after detector simulation, of PYTHIA simulation. The DPS background shape is from event mixing of data [1]. Because the DPS dominates at high mass, the spectrum is fit up to 15 GeV to better constrain its normalization. There is significant combinatorial background for $J/\psi\psi(2S)$, which has three components: $J/\psi\mu^+\mu^-$, $\psi(2S)\mu^+\mu^-$, and $\mu^+\mu^-\mu^+\mu^-$. Its size and shape is obtained from the data by a two dimensional background subtraction method.

Following the $J/\psi J/\psi$ model, the fit includes interfering $X(6900)$ and $X(7100)$ signals, along with SPS, DPS, and combinatorial background shapes. The local significances of individual $X(6900)$ and $X(7100)$ structures are estimated by taking the likelihood ratio of the fit with the likelihood where the peak is absent from the fit, and the $X(6900)$'s and $X(7100)$'s local significances are estimated to be 7.9σ and 4.0σ, respectively. In this evaluation, to evaluate the significance of $X(6900)$ and $X(7100)$, and their consistency with similar peaks in the $J/\psi J/\psi$ spectrum, we constrain the mass and width of both peaks to lie within one standard deviation of the values obtained in the $J/\psi J/\psi$ channel in the fit.

To make an independent measurement of fitting parameters, we remove the constraint, allowing mass and width to float. The results are given in Table 1 under f_{i23}[1], and the corresponding

[1]The asymmetric statistical uncertainties in Table1 for all variables except $\Gamma_{X(6900)}$ are obtained from typical pro-

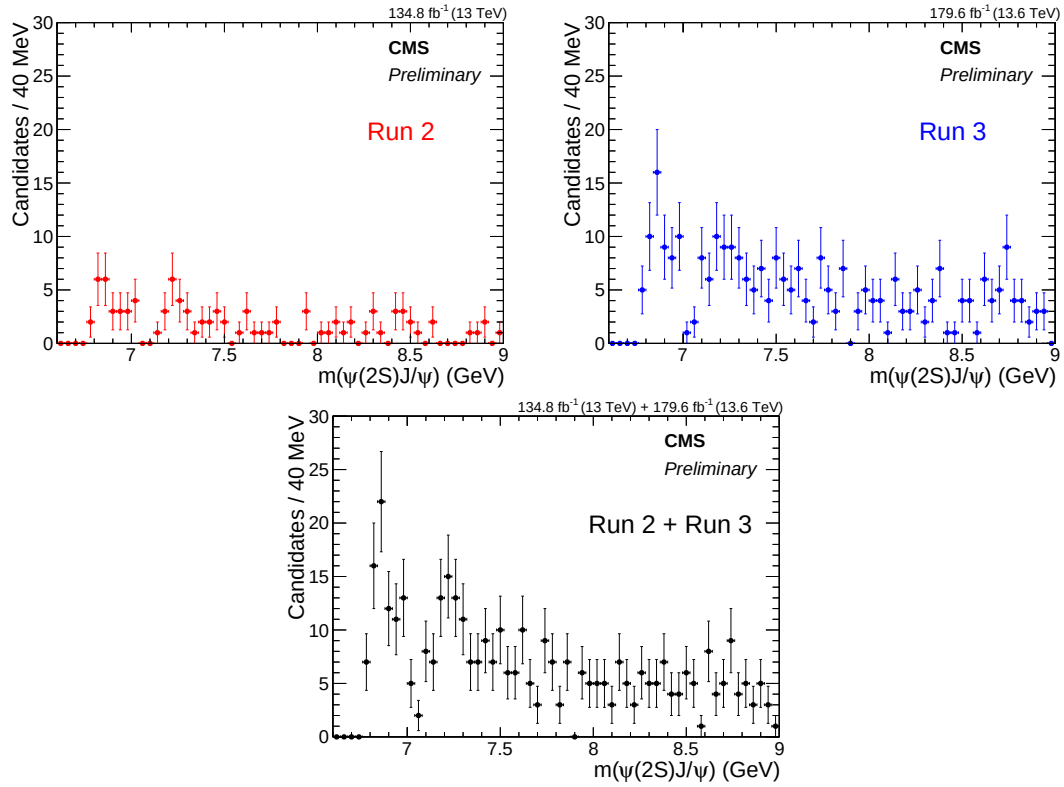

Figure 1: The $J/\psi\psi(2S)$ spectrum under 9 GeV (to make structures more visible) for the Run 2 dataset (upper left), the Run 3 dataset (upper right), and the combined Run 2 + Run 3 dataset (bottom). The number of events below 15 GeV for these three datasets are 139, 415, and 554, respectively.

plots are shown in Figure 2.

Table 1: Fit results of the $J/\psi\psi(2S)$, or $J/\psi J/\psi$, mass spectra. The role of interference, if any, is noted where BW_i represents $X(6600)$, $X(6900)$, and $X(7100)$ for $i = 1, 2, 3$. Masses and widths are in MeV. The top row of numbers is for fit without any constraints from $J/\psi J/\psi$ and that the second row of numbers is the $J/\psi J/\psi$ result for comparison.

Fit	Sample	Interf.		$X(6600)$	$X(6900)$	$X(7100)$
f_{i23}	$J/\psi\psi(2S)$	BW_2, BW_3	m :	—	$6876^{+46+110}_{-29-110}$	7169^{+26+74}_{-52-70}
			Γ :	—	$253^{+290+120}_{-100-120}$	$154^{+110+140}_{-82-160}$
f_{JJ} [1]	$J/\psi J/\psi$	BW_1, BW_2, BW_3	m :	6638^{+43+16}_{-38-31}	6847^{+44+48}_{-28-20}	7134^{+48+41}_{-25-15}
			Γ :	$440^{+230+110}_{-200-240}$	191^{+66+25}_{-49-17}	97^{+40+29}_{-29-26}

The $X(6900)$ and $X(7100)$ parameters may be affected by the (interfering) tail of the sub-threshold $X(6600)$. The effects of this possibility are relegated to the systematic uncertainties.

file scans. The asymmetric uncertainty of $\Gamma_{X(6900)}$ are $^{+670}_{-110}$ MeV due to limited statistics thus $X(7100)$ is absorbed into $X(6900)$. Instead, we first fit with the parabolic approximation ("symmetric uncertainties"), and then a fit is performed where the $X(7100)$ mass and width are fixed to the values from the parabolic fit and the parabolic approximation is released to obtain asymmetric uncertainties of the $X(6900)$ parameters. An uncertainty correction is added to compensate for fixing the $X(7100)$ parameters. Alternate fits are done with $X(7100)$ parameters fixed to $\pm1\sigma$ variations of the values found in the f_{JJ} fit, and these shifts are added in quadrature with the asymmetric errors of the $X(7100)$ constrained fit.

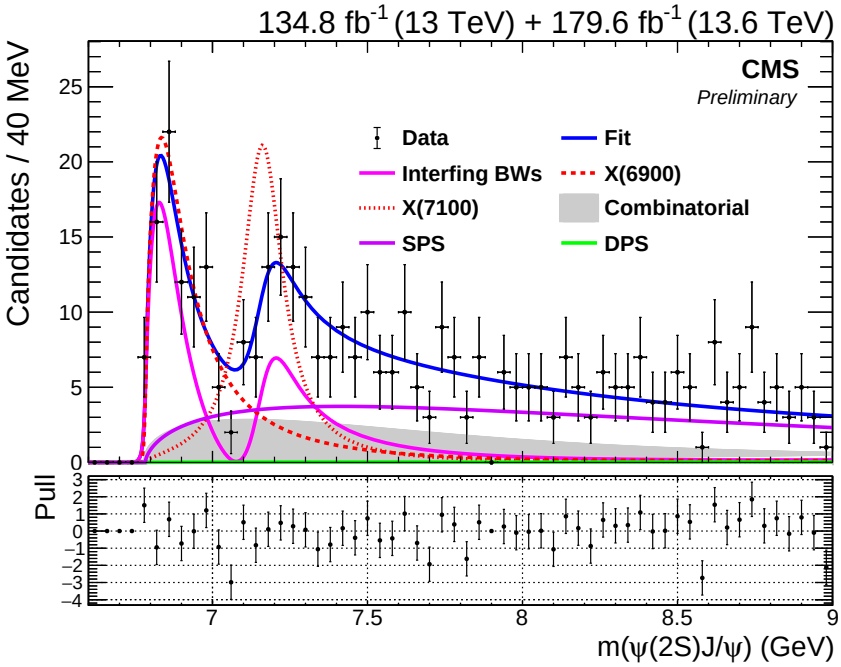

Figure 2: The J/$\psi\psi(2S)$ spectrum with the f_{i23} fit of interfering X(6900) and X(7100) components plus backgrounds (fit extends up to 15 GeV).

Systematic uncertainties on the X(6900) and X(7100) masses and widths for the two-resonance interference fit (f_{i23}) are determined by varying aspects of the fit and taking the largest deviation of a parameter from its nominal value as its systematic uncertainty. Following Ref. [1], the sources of systematic uncertainty considered are: different BW shapes (P- and D-wave, and alternative values for the Blatt–Weisskopf factor [43, 44]); alternative NRSPS and DPS parameterizations; momentum scale; detector mass resolution at different mass point; detector efficiency; combinatorial background shape; and additional peaks.

The systematic uncertainty for the potential effect of the tail of a sub-threshold X(6600) structure is considered by adding an X(6600) BW function to the f_{i23} model for a three-peak interference fit with the X(6600) mass, width, and amplitude relative to the X(6900) fixed to the values from the J/ψJ/ψ fit (f_{JJ}), but with the relative phases allowed to float. Parameter shifts of this fit relative to f_{i23} provide systematic uncertainties due to X(6600) effects.

The principal systematic effects are summarized in Table 2 for f_{i23}. The total systematic uncertainties are the sum in quadrature of the individual contributions.

Here we compare the mass and width of the X(6900) from the J/$\psi\psi(2S)$ channel to those from our J/ψJ/ψ data, and they agree well (f_{i23} vs. f_{JJ} in Table 1). The J/$\psi\psi(2S)$ fit also shows signs of an interference dip around 7100 MeV (Figure 2)—similar to our J/ψJ/ψ data [1]. We conclude that our J/$\psi\psi(2S)$ threshold structure is consistent with X(6900) decays. While other interpretations of our data also cannot be excluded, and the precision of our current data set is low, the concordance between the J/ψJ/ψ and J/$\psi\psi(2S)$ results suggests that other processes do not have a large effect.

As noted, ATLAS has reported a significant excess of events at threshold in the J/$\psi\psi(2S)$ channel [12]. A comparison of our X(6900) results to their model α is not meaningful because the X(6900) mass and width in α were fixed to values from their J/ψJ/ψ data. Our X(6900) central values do not correspond well to model β, especially their large width. On the other hand, our analogous non-interference fit of the X(7100) structure yields a mass and width of 7240 ± 19

Table 2: Dominant contributions to the systematic uncertainties on the X(6900) and X(7100) masses and widths, in MeV, for fit f_{i23}. The "Total" is the sum in quadrature of all components, including unlisted non-dominant contributions.

Dominant sources	$M_{X(6900)}$	$\Gamma_{X(6900)}$	$M_{X(7100)}$	$\Gamma_{X(7100)}$
Signal shape	± 29	± 79	± 22	± 131
NRSPS shape	± 14	± 54	± 14	± 29
Combinatorial background shape	± 15	± 51	± 15	± 20
Mass resolution	± 5	± 7	± 5	± 9
Efficiency	± 7	± 27	± 7	± 10
Add X(6600) peak	± 104	± 14	± 61	± 31
Fitter bias	$^{+9}_{-11}$	$^{+43}_{-37}$	$^{+29}_{-14}$	$^{0}_{-80}$
Total	$^{+110}_{-110}$	$^{+120}_{-120}$	$^{+74}_{-70}$	$^{+140}_{-160}$

and 62 ± 44 MeV and agrees well with the 7220 MeV peak of model α.

ATLAS refrained from specifically ascribing their excess to $X(6900) \to J/\psi\psi(2S)$ decays out of caution that the details of their structure could not be discerned directly from their data, and other interpretations could not be excluded, e.g., multiple non-interfering resonances, reflection effects, and threshold enhancements [12].

In summary, using 314 fb^{-1} of collisions recorded in 2016-2018 and 2022-2024, CMS observes an excess in $J/\psi\psi(2S)$ near threshold well above five standard deviations (5σ), consistent with $X(6900) \to J/\psi\psi(2S)$. There is evidence of an $X(7100) \to J/\psi\psi(2S)$ signal with 4.0σ local significance. These excesses are consistent with similar ones observed in the $J/\psi J/\psi$ mass spectrum identified by CMS [1], LHCb [11] and ATLAS [12]. Recently CMS reported an angular analysis of the $X \to J/\psi J/\psi$ decay characteristics and found the J^{PC} quantum numbers of the X family is most likely 2^{++} [45].

References

[1] CMS Collaboration, "New structures in the $J/\psi J/\psi$ mass spectrum in proton-proton collisions at $\sqrt{s} = 13$ TeV", *Phys. Rev. Lett.* **132** (2024) 111901, doi:10.1103/PhysRevLett.132.111901, arXiv:2306.07164.

[2] CMS Collaboration, "Observation of a family of all-charm tetraquark candidates at the lhc", *CMS PAS-BPH-24-003* (2025).

[3] R. Zhu, "Fully-heavy tetraquark spectra and production at hadron colliders", *Nuclear Physics B* **966** (2021) 115393, doi:10.1016/j.nuclphysb.2021.115393, arXiv:2010.09082.

[4] R. Tiwari, D. P. Rathaud, and A. K. Rai, "Spectroscopy of all charm tetraquark states", *Indian J Phys* **97** (2023) 943–954, doi:10.1007/s12648-022-02427-8.

[5] F. Zhu, G. Bauer, and K. Yi, "Experimental road to a charming family of tetraquarks and beyond", *Chinese Physics Letters* **41** (dec, 2024) 111201, doi:10.1088/0256-307X/41/11/111201.

[6] Belle Collaboration Collaboration, "Observation of a narrow charmoniumlike state in exclusive $B^{\pm} \to K^{\pm}\pi^{+}\pi^{-}j/\psi$ decays", *Phys. Rev. Lett.* **91** (Dec, 2003) 262001, doi:10.1103/PhysRevLett.91.262001.

[7] BESIII Collaboration, "Observation of a charged charmoniumlike structure in $e^+e^- \to \pi^+\pi^- J/\psi$ at $\sqrt{s}$=4.26 GeV", *Phys. Rev. Lett.* **110** (2013) 252001, doi:10.1103/PhysRevLett.110.252001.

[8] Belle Collaboration, "Study of $e^+e^- \to \pi^+\pi^- J/\psi$ and observation of a charged charmoniumlike state at Belle", *Phys. Rev. Lett.* **110** (2013) 252002, doi:10.1103/PhysRevLett.110.252002.

[9] A. Ali, L. Maiani, and A. D. Polosa, "Multiquark Hadrons". Cambridge University Press, 2019.

[10] H.-X. Chen et al., "An updated review of the new hadron states", *Reports on Progress in Physics* **86** (2023) 026201, doi:10.1088/1361-6633/aca3b6, arXiv:2204.02649.

[11] LHCb Collaboration, "Observation of structure in the J/ψ-pair mass spectrum", *Sci. Bull.* **65** (2020), no. 23, 1983–1993, doi:10.1016/j.scib.2020.08.032, arXiv:2006.16957.

[12] ATLAS Collaboration, "Observation of an excess of di-charmonium events in the four-muon final state with the ATLAS detector", *Phys. Rev. Lett.* **131** (2023) 151902, doi:10.1103/PhysRevLett.131.151902.

[13] N. Brambilla et al., "The xyz states: Experimental and theoretical status and perspectives", *Physics Reports* **873** (2020) 1–154, doi:https://doi.org/10.1016/j.physrep.2020.05.001.

[14] M. Nielsen et al., "Supersymmetry in the Double-Heavy Hadronic Spectrum", *Phys. Rev. D* **98** (2018) 034002, doi:10.1103/PhysRevD.98.034002, arXiv:1805.11567.

[15] M. Nielsen and S. J. Brodsky, "Hadronic superpartners from a superconformal and supersymmetric algebra", *Phys. Rev. D* **97** (2018) 114001, doi:10.1103/PhysRevD.97.114001, arXiv:1802.09652.

[16] X. Jin, Y. Xue, H. Huang, and J. Ping, "Full-heavy tetraquarks in constituent quark models", *Eur. Phys. J. C* **80** (2020), no. 11, 1083, doi:10.1140/epjc/s10052-020-08650-z, arXiv:2006.13745.

[17] R. Zhu, "Fully-heavy tetraquark spectra and production at hadron colliders", *Nucl. Phys. B* **966** (2021) 115393, doi:10.1016/j.nuclphysb.2021.115393, arXiv:2010.09082.

[18] B.-D. Wan and C.-F. Qiao, "Gluonic tetracharm configuration of $X(6900)$", *Phys. Lett. B* **817** (2021) 136339, doi:10.1016/j.physletb.2021.136339, arXiv:2012.00454.

[19] W.-L. Wu, Y.-K. Chen, L. Meng, and S.-L. Zhu, "Benchmark calculations of fully heavy compact and molecular tetraquark states", *Phys. Rev. D* **109** (Mar, 2024) 054034, doi:10.1103/PhysRevD.109.054034.

[20] X.-K. Dong et al., "Coupled-channel interpretation of the LHCb double-J/ψ spectrum and hints of a new state near the $J/\psi J/\psi$ threshold", *Phys. Rev. Lett.* **126** (Mar, 2021) 132001, doi:10.1103/PhysRevLett.126.132001.

[21] F.-K. Guo, X.-H. Liu, and S. Sakai, "Threshold cusps and triangle singularities in hadronic reactions", *Prog. Part. Nucl. Phys.* **112** (2020) 103757, doi:10.1016/j.ppnp.2020.103757, arXiv:1912.07030.

[22] C. Gong et al., "Nature of X(6900) and its production mechanism at LHCb", *Physics Letters B* **824** (2022) 136794, doi:https://doi.org/10.1016/j.physletb.2021.136794.

[23] J.-Z. Wang, X. Liu, and T. Matsuki, "Fully-heavy structures in the invariant mass spectrum of $J/\psi\psi(3686)$, $J/\psi\psi(3770)$, $\psi(3686)\psi(3686)$, and $J/\psi\Upsilon(1S)$ at hadron colliders", *Phys. Lett. B* **816** (2021) 136209, doi:10.1016/j.physletb.2021.136209, arXiv:2012.03281.

[24] CDF Collaboration, "Evidence for a narrow near-threshold structure in the $J/\psi\phi$ mass spectrum in $B^+ \to J/\psi\phi K^+$ decays", *Phys. Rev. Lett.* **102** (2009) 242002, doi:10.1103/PhysRevLett.102.242002.

[25] CDF Collaboration, "Observation of the $Y(4140)$ structure in the $J/\psi\phi$ mass spectrum in $B^\pm \to J/\psi\phi K^\pm$ decays", *Mod. Phys. Lett. A* **32** (2017), no. 26, 1750139, doi:10.1142/S0217732317501395, arXiv:1101.6058.

[26] CMS Collaboration, "The CMS Experiment at the CERN LHC", *JINST* **3** (2008) S08004, doi:10.1088/1748-0221/3/08/S08004.

[27] Y. Gao et al., "Spin determination of single-produced resonances at hadron colliders", *Phys. Rev. D* **81** (Apr, 2010) 075022, doi:10.1103/PhysRevD.81.075022.

[28] S. Bolognesi et al., "Spin and parity of a single-produced resonance at the LHC", *Phys. Rev. D* **86** (Nov, 2012) 095031, doi:10.1103/PhysRevD.86.095031.

[29] I. Anderson et al., "Constraining anomalous HVV interactions at proton and lepton colliders", *Phys. Rev. D* **89** (Feb, 2014) 035007, doi:10.1103/PhysRevD.89.035007.

[30] A. V. Gritsan, R. Röntsch, M. Schulze, and M. Xiao, "Constraining anomalous higgs boson couplings to the heavy-flavor fermions using matrix element techniques", *Phys. Rev. D* **94** (Sep, 2016) 055023, doi:10.1103/PhysRevD.94.055023.

[31] A. V. Gritsan et al., "New features in the JHU generator framework: Constraining Higgs boson properties from on-shell and off-shell production", *Physical Review D* **102** (2020), no. 5, doi:10.1103/physrevd.102.056022.

[32] T. Sjöstrand, S. Mrenna, and P. Skands, "A brief introduction to PYTHIA 8.1", *Computer Physics Communications* **178** (2008), no. 11, 852–867, doi:10.1016/j.cpc.2008.01.036.

[33] H. Jung et al., "The CCFM monte carlo generator CASCADE Version 2.2.03", *The European Physical Journal C* **70** (2010), no. 4, 1237–1249, doi:10.1140/epjc/s10052-010-1507-z.

[34] H.-S. Shao, "Helac-onia: An automatic matrix element generator for heavy quarkonium physics", *Computer Physics Communications* **184** (2013) doi:10.1016/j.cpc.2013.05.023.

[35] J.-P. Lansberg and H.-S. Shao, "J/ψ-pair production at large momenta: Indications for double parton scatterings and large α_s^5 contributions", *Physics Letters B* **751** (2015) 479–486, doi:https://doi.org/10.1016/j.physletb.2015.10.083.

[36] J.-P. Lansberg and H.-S. Shao, "Production of $J/\psi + \eta_c$ versus $J/\psi + J/\psi$ at the LHC: Importance of real α_s^5 corrections", *Physical Review Letters* **111** (2013) doi:10.1103/physrevlett.111.122001.

[37] H.-S. Shao, "Helac-onia 2.0: An upgraded matrix-element and event generator for heavy quarkonium physics", *Computer Physics Communications* **198** (2016) 238–259, doi:https://doi.org/10.1016/j.cpc.2015.09.011.

[38] GEANT4 Collaboration, "GEANT4–a simulation toolkit", *Nucl. Instrum. Meth. A* **506** (2003) 250–303, doi:10.1016/S0168-9002(03)01368-8.

[39] CMS Collaboration, "The CMS trigger system", *JINST* **12** (2017), no. 01, P01020, doi:10.1088/1748-0221/12/01/P01020, arXiv:1609.02366.

[40] CMS Collaboration, "Performance of CMS muon reconstruction in pp collision events at $\sqrt{s} = 7$ TeV", *JINST* **7** (2012) P10002, doi:10.1088/1748-0221/7/10/P10002, arXiv:1206.4071.

[41] G. Punzi, "Sensitivity of searches for new signals and its optimization", *eConf* **C030908** (2003) MODT002, arXiv:physics/0308063.

[42] Particle Data Group Collaboration, "Review of Particle Physics", *Progress of Theoretical and Experimental Physics* **2022** (08, 2022) 083C01, doi:10.1093/ptep/ptac097.

[43] C. Q. F. Von Hippel, "Centrifugal-Barrier Effects in Resonance Partial Decay Widths, Shapes, and Production Amplitudes", *Phys. Rev. D* **52** (1972) 624, doi:10.1103/PhysRevD.5.624.

[44] S. U. Chung, "Helicity-coupling amplitudes in tensor formalism", *Phys. Rev. D* **48** (Aug, 1993) 1225–1239, doi:10.1103/PhysRevD.48.1225.

[45] CMS Collaboration, "Spin and symmetry properties of all-charm tetraquarks", *CMS PAS-BPH-24-002* (2025).